Phys Chem Minerals (1994) 20:521–530

PHYSICS AND CHEMISTRY OF MINERALS

Microstructural Defects in Experimentally Shocked Diopside: A TEM Characterization

Hugues Leroux[1], Jean Claude Doukhan[1], and Falko Langenhorst[1,2]

[1] Laboratoire de Structure et Propriétés de l'Etat Solide (URA CNRS 234), Université des Sciences et Technologies de Lille, F-59655 Villeneuve d'Ascq-Cedex, France
[2] Institut für Planetologie, Wilhelm-Klemm-Str. 10, Universität Münster, D-48149 Münster, Germany

Received January 25, 1993 / Revised, accepted October 25, 1993

Abstract. Transmission electron microscopy was used for characterizing the defect microstructure induced by shock experiments in a single crystal of diopside. The shock-induced defects found in the crystal can be divided in four distinct types:

1) A high density and pervasive distribution of dislocations in glide configuration (glide systems (100)[001], {110}[001] and (100)[010]).

2) Mechanical twin lamellae, mostly parallel to (100), the (001) twin lamellae are less abundant.

3) Straight and narrow amorphous lamellae parallel to a few planes with low crystallographic indices (the $(33\bar{1})$ lamellae are the most abundant but $(22\bar{1})$ and (110) lamellae are also present).

4) Heterogeneously distributed tiny molten zones (3 to 20 μm size) which, after cooling, appear as a glass with a chemical composition very close to the one of the original diopside.

The present TEM study reveals that the defect microstructure in shocked diopside consists of a large variety of shock-induced defects. Especially, the amorphous PDFs which were never observed in statically deformed diopside seem to be an important characteristic microstructural defects in shocked silicate minerals. Although the presence of amorphous PDFs is not yet confirmed for naturally shocked clinopyroxene, we strongly suggest that these features can serve as a diagnostic tool for recognizing impact phenomena on all planetary bodies of our solar system.

Introduction

TEM is a privileged tool for investigating the defect microstructures induced by shock deformation in minerals. This technique has already been employed to study naturally and experimentally shocked silicates such as quartz, olivine, pyroxene and feldspar. The most usual shock-induced defects are planar fractures, mechanical twins, kink bands, amorphous lamellae, high pressure polymorphs and molten zones. In the case of quartz which is the mineral in which shock-induced defects have been mostly studied, the prominent defects are the so-called "Planar Deformation Features" (PDFs) which, in almost all cases, appear be straight and narrow amorphous lamellae parallel to a few rhombohedral planes $\{10\bar{1}n\}$ with n=1, 2, 3 and 4 (Kieffer et al. 1976; Gratz 1984; Ashworth and Schneider 1985; Gratz et al. 1988; Goltrant et al. 1991, 1992). In olivine, the prominent shock defects are deformation bands, planar fractures and glass pockets (Ashworth and Barber 1975a, 1977; Jeanloz et al. 1977; Dodd and Jarosewich 1979; Jeanloz 1980; Schaal 1982; Ashworth 1985; Stöffler et al. 1991). Planar deformation features and the so-called diaplectic glass or maskelynite are common shock effects in feldspars (Stöffler 1972; Stöffler et al. 1991 and references therein). The prominent shock-induced defects in orthopyroxenes consist of thin lamellae of clinoenstatite ($P2_1/c$) parallel to the (100) plane (Ashworth and Barber 1975b; Ashworth 1985) which result from the pseudomartensitic transformation orthoenstatite ⇒ clinoenstatite (Coe and Kirby 1975; Kirby 1976).

The case of diopside still is poorly documented. It is, however, one of the minerals commonly found in stony meteorites. It may be thought that if correctly calibrated, shocked diopside could be used as a thermomechanical marker of the structure and the amplitude of natural shock. Indeed, owing to its low crystallographic symmetry, it is expected to exhibit a variety of shock defects and because its rate of recovery or recrystallization is low, the probability for overprinting of such defects by post-shock thermal events (annealing, recrystallization ...) is appreciably lower than in other silicates like olivine for instance. Shock experiments on diopside single crystals have been shown to predominantly induce (001) thin twin lamellae (Hornemann and Müller 1971). (100) twins are also found, and coexist with the (001) ones in Shergotty meteorite (Müller 1993) and in strongly shocked meteorites (Ashworth 1985). However, Nord

Correspondence to: H. Leroux

and McGee (1979) and Ashworth (1980) report only (100) twins in a weakly shocked lunar augite and in mildly shocked chondritic diopside, respectively. Clinopyroxene has been shown to become amorphized at shock pressures above 50 GPa (Christie and Ardell 1976). Data analysis from shock compressed diopside up to 145 GPa (Svendsen and Ahrens 1983, 1990; Liu 1987) suggest that high pressure phases could form consistent with either a model oxide ($CaO+MgO+SiO_2$) and/or a perovskite assemblage ($CaSiO_3-MgSiO_3$ or possibly $CaMgSi_2O_6$ perovskites). No planar deformation features similar to the ones detected in quartz were detected in shocked pyroxenes so far.

Experimental

A high explosive technique, previously described by Langenhorst et al. (1992), was used to shock a preheated diopside single crystal parallel to the (100)-face to a peak pressure of 45 GPa. The crystal was collected at Daun (Eifel, Germany). Its mean composition $Mg_{0.77}Ca_{0.89}Fe_{0.23}Na_{0.05}Si_{1.83}O_6$ was determined by electron microprobe (cation stochiometry referring to 6 oxygen atoms). A disk, 0.5 mm thick and 10 mm in diameter, was cut parallel to the (100) plane and put in an ARMCO-steel container. The sample container was externally preheated in a furnace at 640° C prior to the shock experiment. Thereafter, it was impacted by a high explosive driven flyer plate (Hornemann and Müller 1971). Due to actual handling procedures the temperature directly before the passage of the shock wave was 630 ± 5° C. According to the graphical impedance method the shock pressure of 45 GPa was calculated.

Optical and X-ray Observations

At the optical microscope the starting material shows a few fractures and weathered regions, most of which were aligned along planes (healed fracture surfaces?). Measurements of birefringence and optical axial angles were performed on our material before and after shock with a Medenbach microrefractometer spindle stage (Medenbach 1985). Compared to unshocked material, the optical parameters of the shocked diopside remain unchanged. The data reported in Table 1 show that both birefringence and the optical axial angle, remain unchanged within the uncertainty of the experiments. Differences in the optical behaviour are, however, detected between unshocked and shocked materials. Whereas the unshocked reference material shows under crossed nicols sharp extinction, the shocked material displays strong mosaicism easily recognizable by its irregular extinction behaviour.

Table 1. Birefringence n_z-n_x, optic axis angle $2V_z$, and the according 2σ errors of unshocked (0 GPa) and shocked (45 GPa) diopside

P(GPa)	$2V_z$(°)	n_z-n_x
0	64.1 ± 1.1	0.029 ± 1
45	63.7 ± 2.3	0.028 ± 1

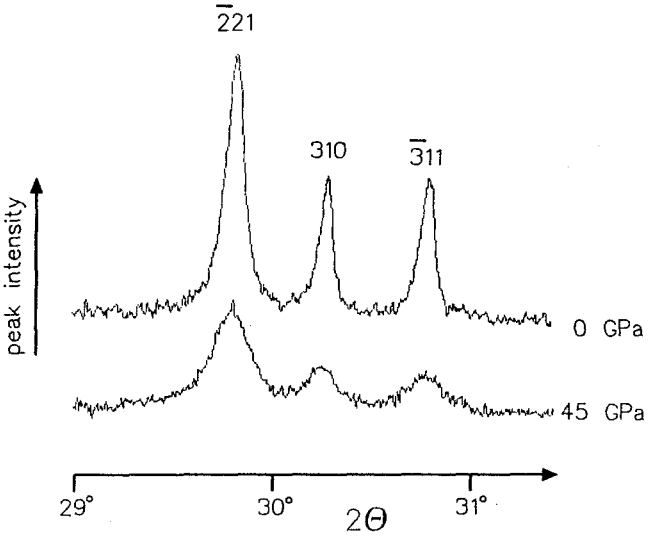

Fig. 1. X-ray spectrum of unshocked and shocked diopside in the 2θ range from 29.0 to 31.5°. The peaks of the shocked diopside display a lower intensity and a broader half width

X-ray diffraction diagrams recorded with a Guinier-Jagodzinski powder diffraction camera show line broadening and lowering of peak intensities for the shocked material as compared to the unshocked one (Fig. 1). Such features are found in many X-ray spectra recorded on shocked silicates. In contrast to the case of quartz (Schneider et al. 1984) no line shifts are detected. The lattice parameters of shocked diopside appear identical to the ones of unshocked diopside within the uncertainties of the measurements (Table 2). The line broadening must thus result from a severe grain size decrease (Klug and Alexander 1974).

TEM Investigations

TEM investigations on the reference material reveal a low defect content, the major defects are dislocations with a density $<10^{10}$ m^{-2}. Most of them are organized in subgrain boundaries (Fig. 2). Such a microstructure is consistent with its thermomechanical history (deformation by high temperature creep with a low stress and a low strain rate). No twins, precipitates of a foreign phase, or exsolution were detected by TEM. In contrast, in the shocked material one observes a very large density of defects as shown on Fig. 3. Electron diffraction pat-

Table 2. Lattice parameters and 2σ errors of unshocked (0 GPa) and shocked (45 GPa) diopside determined by the Guinier-Jagodzinski method

P(GPa)	a(Å)	b(Å)	c(Å)	V(Å^3)	β(°)
0	9.7478 ± 18	8.8895 ± 19	5.2825 ± 9	439.89 ± 9	106.056 ± 15
45	9.7526 ± 32	8.8956 ± 34	5.2817 ± 16	440.31 ± 16	106.070 ± 28

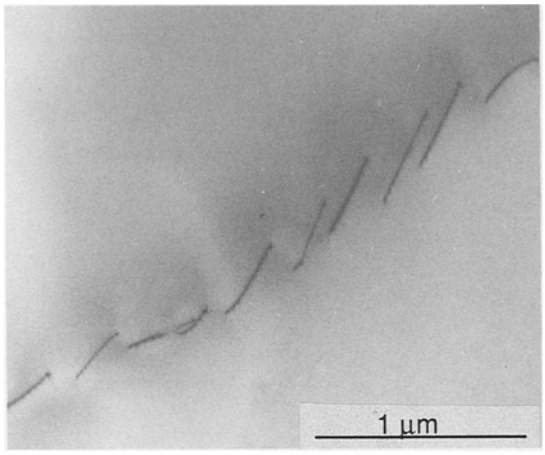

Fig. 2. Typical defect microstructure in the as-received material. Most dislocations are organized in subgrain boundaries (*bright field*)

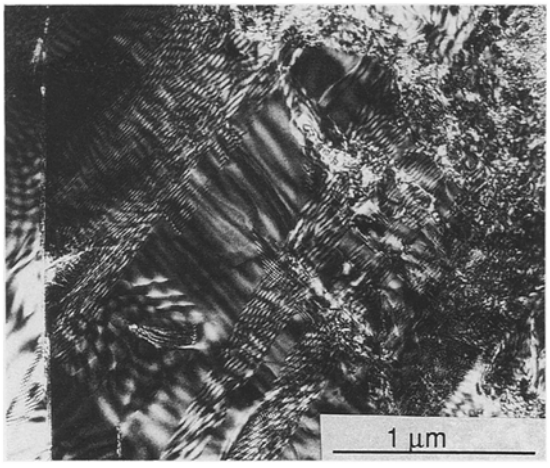

Fig. 3. Dark field micrograph showing a general view of the shock-induced defects. They consist of fractures, a large and pervasive density of dislocations and other extended defects

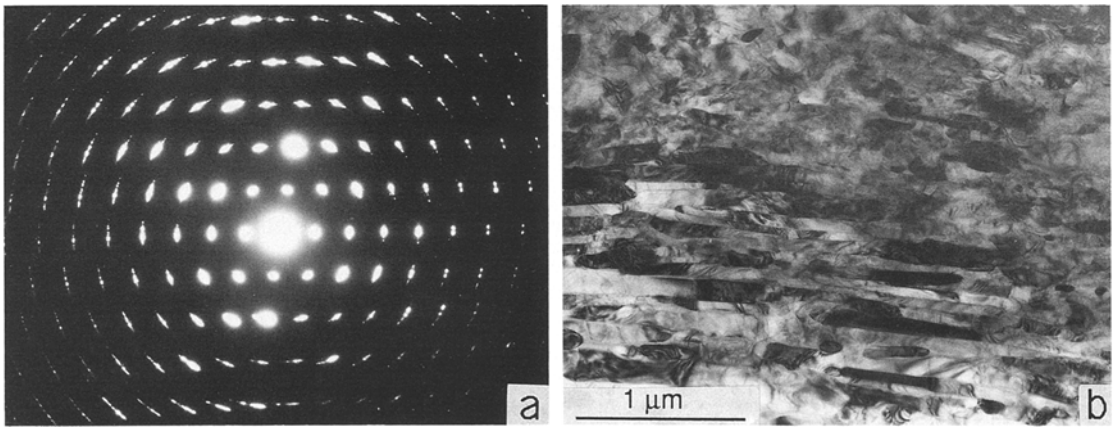

Fig. 4. **a** Diffraction pattern with the diffraction spots exhibiting a marked asterism due to the mosaic structure of the diffracting material. **b** Corresponding diffracting area (*bright field*)

terns recorded on small areas of the order of $\approx 10\ \mu m^2$ present a marked asterism (Fig. 4) which clearly stems from the shock-induced "mosaic" structure of the material (the crystal is divided in small zones or blocks slightly and mutually misoriented). Moreover, we observed and characterized a number of shock-induced defects. For the sake of simplicity they are regrouped here below in four major types. 1) Dislocations. 2) Twin lamellae. 3) Melt pockets. 4) Straight and narrow planar defects parallel to low crystallographic index planes.

1) Dislocations

Shock-induced dislocations are pervasive with a high density (order of $5.10^{13}\ m^{-2}$) (Fig. 5). We were able to fully characterize a number of them and we only find the Burgers vectors b and c. These dislocations present no preferred orientations, they are smoothly curved but they all lie in their respective glide planes. They belong to the following glide systems (100)[001] (predominant), {110}[001] and (100)[010]. Numerous Frank-Read sources are also observed (Fig. 5c) suggesting that most dislocations glided over quite short distances. As a result, these shock-induced dislocations generated no appreciable amount of plastic strain, in agreement with the very short time of the shock experiment. It is to be noted that the glide systems $\{110\}1/2<110>$ which have recently been characterized as the easiest glide systems at high temperature (Ingrin et al. 1991) are not observed here.

2) Twins

A high density of thin twin lamellae is observed. They are heterogeneously distributed without no twins in some regions while in others their mean spacing can be as low as 0.1 μm (Fig. 6a). Twin lamellae were characterized by their orientation, by their extra-spots in diffraction patterns (Fig. 6b and 6c) and by their specific fringe patterns in diffraction contrast experiments. Most

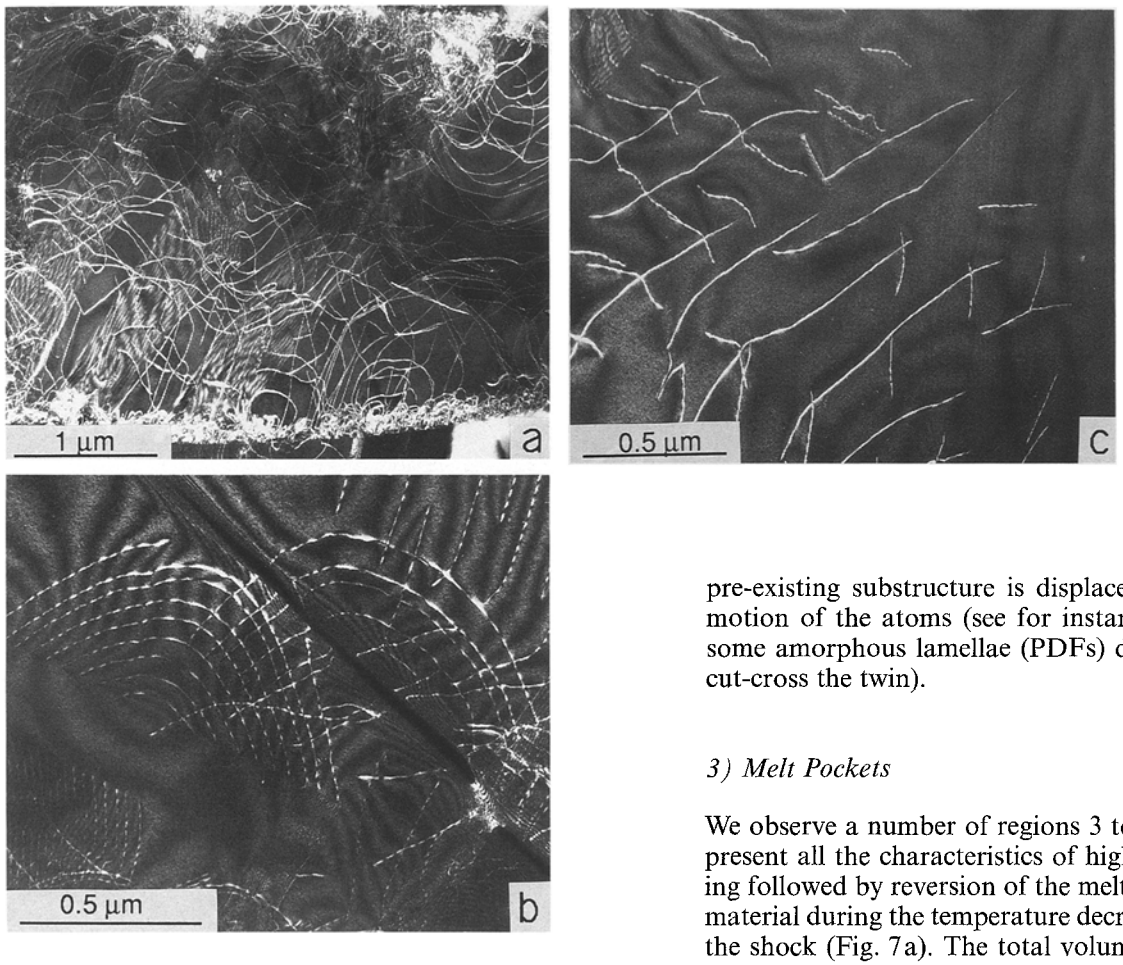

Fig. 5a–c. Dark field micrographs. **a** High and pervasive density of dislocations. A large number seem to be nucleated on the fracture edge in the *lower part* of the micrograph. Such dislocations lie in the (100) foil plane and belong to the (100)[001] glide system. **b** The other dislocations with a zig-zag contrast belong to the glide systems {110} [001]. **c** Numerous dislocation configurations clearly indicate that Frank-Read sources were activated

of them are (100) twins but a few (001) twin lamellae are detected. Both types of twins must be mechanical ones, and in the case of the (100) twins, we observe at their tips (Fig. 6d) the partial dislocations which generated the twins (Kirby and Christie 1977). Standard contrast analysis shows that the Burgers vector of these "twin" dislocations is parallel to c with a modulus close to $^1/_2$ [001]. Such twin dislocations are often curved. They might have been nucleated by a mechanism similar to the one of a Frank-Read source with the successive $^1/_2$ [001] partial dislocations nucleated in adjacent (100) planes. Such a mechanism for generating dislocation-induced mechanical twinning is not conventional, but shock induced deformation is not conventional either.

(001) twins are much less abundant and they are thicker than the (100) ones (thickness of 0.1 to 0.5 μm to be compared to less than 50 nm for the (100) twin lamellae). They seem to extend through the whole crystal. Furthermore, one never detects partial dislocations in the boundaries of these (001) twin lamellae. The (001) twin appears as a kinking lamellar region, where the pre-existing substructure is displaced by a cooperative motion of the atoms (see for instance Fig. 8c showing some amorphous lamellae (PDFs) deflected where they cut-cross the twin).

3) Melt Pockets

We observe a number of regions 3 to 20 μm wide which present all the characteristics of high temperature melting followed by reversion of the melt product in a glassy material during the temperature decrease which followed the shock (Fig. 7a). The total volumic fraction of these melt regions reaches a value of the order of 1%. Diffraction patterns of these glassy zones show the weakly contrasted concentric rings typical of an amorphous phase. Within the glass one detects a number of tiny spheric holes or bubbles, which could result from local vaporization during shock compression. Their diameter ranges from 0.02 to 0.5 μm. Along the rims of the glassy regions, at the border with the crystalline matrix, tiny crystallites are detected. Their mean size is of the order of 0.1 μm and the diffraction patterns performed on this polycrystalline material are consistent with the diopside structure. Microanalyses performed on these glassy regions reveal compositions very similar to the one of the original diopside. A melting process thus occurs in some restricted areas in our sample, indicating that the shock pressure is accompanied by a high and heterogeneous temperature pulse able to locally raise the temperature up to values appreciably larger than the melting temperature at room pressure ($\approx$1320° C for the present composition). We also observe narrow and elongated amorphous regions with a width of the order of 1 to 3 μm (Fig. 7b). They present no specific orientation i.e. they do not seem to be crystallographically controlled. The occurrence of small voids or gaseous bubbles in their middle as well as tiny diopside crystallites (size 0.05 μm to 0.5 μm) along their rims confirm the hypothesis that such veins also result from localized melting. Finally it is to be mentioned that similar concentric rings typical of an amorphous material are also detected on a number

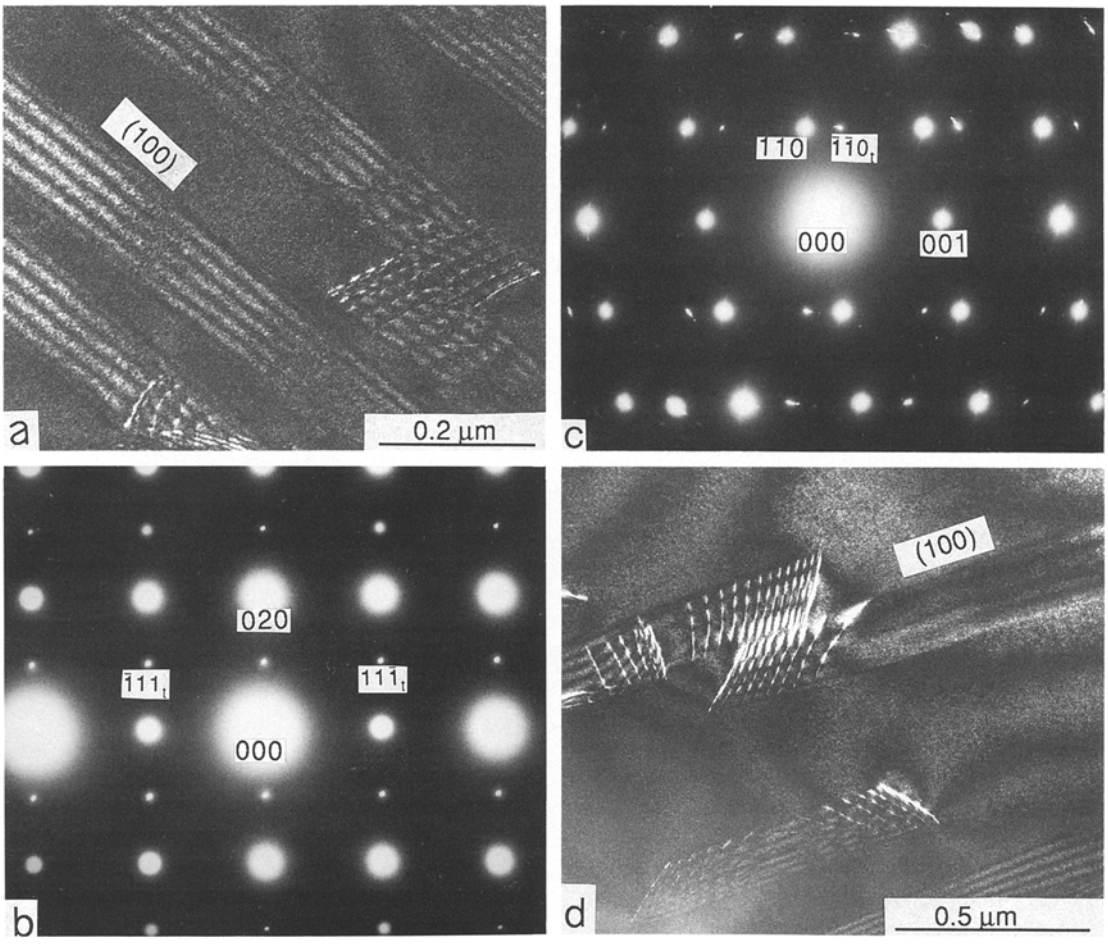

Fig. 6. **a** Area with a large density of (100) twin lamellae (*dark field*). **b** Diffraction pattern (zone axis 100) on matrix plus (100) twins. **c** Diffraction pattern (zone axis $1\bar{1}0$) on matrix plus (001) twins. The refections according to the mirror twin law are present. **d** Partial dislocations at the tips of (100) twin lamellae (*dark field*)

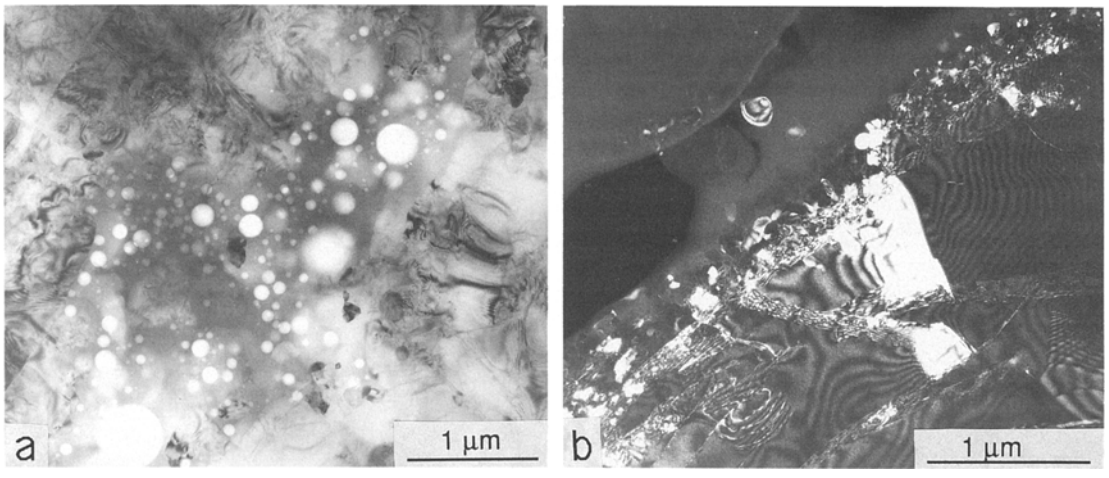

Fig. 7. **a** Glassy zone resulting from localized melt. Note the tiny spheric holes which may contain gas or result from differential thermal contraction between crystalline matrix and glass (*bright field*). **b** Glass vein with small crystallites of diopside along its rim (*dark field*)

of diffraction patterns recorded on regions which, in bright field, appear as crystalline material (these rings are however very weakly contrasted). Some small amorphous regions must thus occur within this material too, but it was not possible to detect them in bright field micrographs, presumably because they are very tiny regions exhibiting a weak contrast and this contrast must be overprinted by the one of other lattice defects (dislocations, twin lamellae ...) which are present in the ame areas with quite a large density.

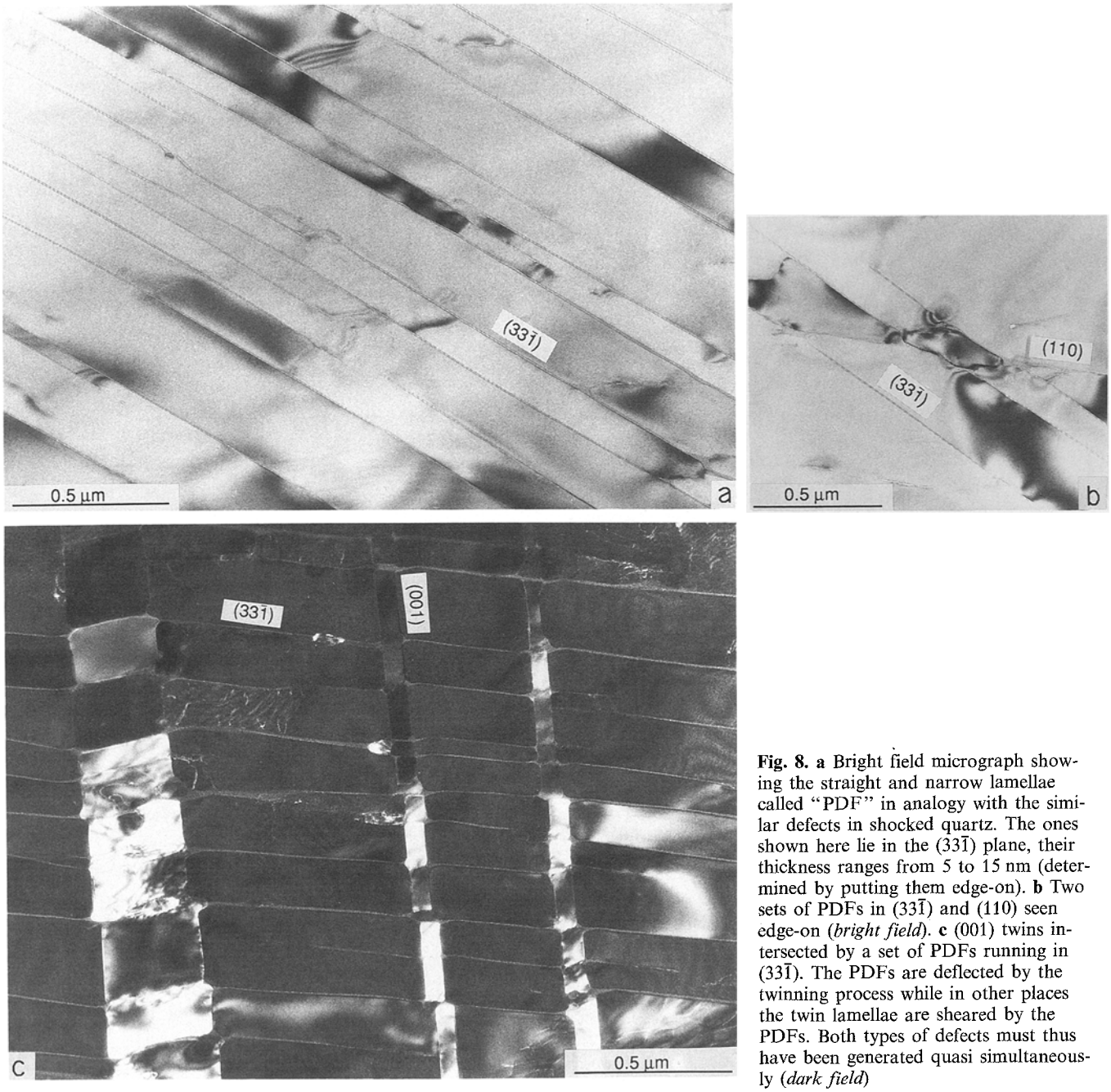

Fig. 8. a Bright field micrograph showing the straight and narrow lamellae called "PDF" in analogy with the similar defects in shocked quartz. The ones shown here lie in the (33$\bar{1}$) plane, their thickness ranges from 5 to 15 nm (determined by putting them edge-on). **b** Two sets of PDFs in (33$\bar{1}$) and (110) seen edge-on (*bright field*). **c** (001) twins intersected by a set of PDFs running in (33$\bar{1}$). The PDFs are deflected by the twinning process while in other places the twin lamellae are sheared by the PDFs. Both types of defects must thus have been generated quasi simultaneously (*dark field*)

4) Planar Deformation Features (PDFs)

The term "Planar Deformation Feature" or PDF was proposed in 1989 at the Snow Bird conference for designating the typical extended defects which are systematically detected in shocked quartz (Grieve et al. 1990). We use here the same term to designate the straight and narrow extended defects which we detect in shocked diopside because of their similar appearance in both minerals. In the present case PDFs occur parallel to a few specific planes with low crystallographic indices. {33$\bar{1}$} is the predominant plane, but {22$\bar{1}$} and {110} are also observed (Fig. 8a and b). These PDFs are pervasive and rather homogeneously distributed with a mean spacing between parallel sets of the order of 0.1 to 0.5 μm. Although most of them run through the whole crystal, some stop in the bulk, allowing their tip to be investigated in detail. In some cases this tip is surrounded by a large density of dislocations, in other cases the PDF end on an open fracture. When such PDFs intersect other shock defects like twins or dislocations, offsets are clearly detected, indicating that, in contrast with the case of quartz, PDFs in diopside have a shearing character. For instance Fig. 8c shows the intersection of a set of PDFs in (33$\bar{1}$) with a set of (001) twin lamellae. As twins also present a shearing character, either one or the other extended defect (PDF or twin) is sheared by the other, depending on which type was generated

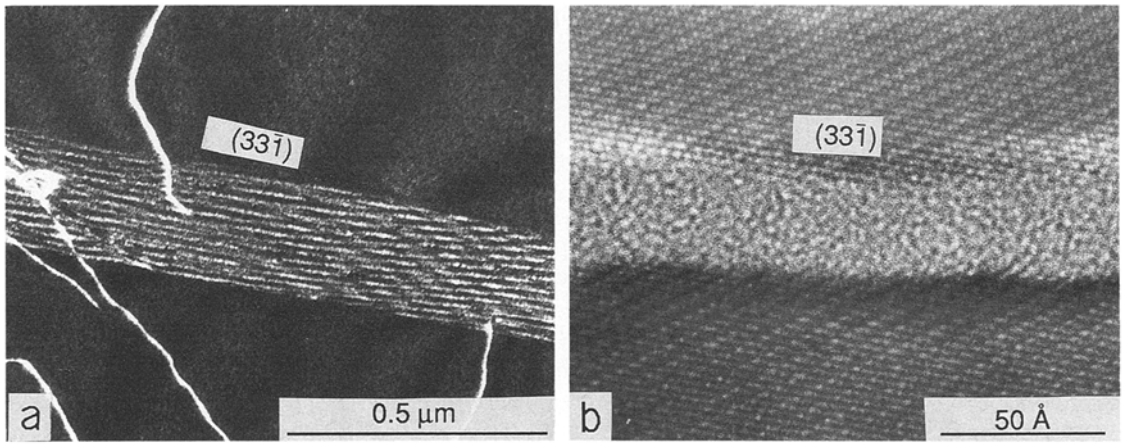

Fig. 9. a Irregular fringe pattern of inclined PDFs. The fringes result from the wedge shaped crystalline rims bounding the PDFs and the interferences observed indicate a slight misorientation between both sides of a given PDF (*dark field*). **b** High resolution imaging of PDFs showing that they apparently consist of a thin lamella of amorphous material

first by the shock wave and was subsequently sheared by the other extended defect. As a result their intersections may exhibit quite a complicated structure (Fig. 8c).

These PDFs are very narrow and can be detected and characterized only by TEM. We determined their habit planes and their thicknesses by tilting the specimen in such a way that they were put edge-on. As a general trend, they are extremely narrow with thicknesses ranging from 5 to 15 nm. In diffraction contrast experiments in two beam conditions inclined PDFs present an irregular fringe pattern indicating that they cannot be assigned to the usual stacking faults. The fringes rather result from the crystalline wedges bounding the PDFs (Fig. 9a). In some cases we were able to observe the fringe systems of both crystalline rims of a given PDF. In these cases both sets of fringes form interferences, indicating that a slight misorientation occurs between both crystalline rims. Slight misorientations are also detected on bright field micrographs through the different contrasts presented by adjacent crystalline rims (see Fig. 8a). Therefore, in contrast to the case of quartz, the process of PDF nucleation in shocked diopside separates the crystal in two parts which are at the same time sheared and slightly rotated one versus the other. Finally we also used high resolution imaging for elucidating the fine structure of these defects (Fig. 9b). PDFs obviously consist of thin amorphous lamellae with a thickness which slightly varies all along the PDF. The formation during the shock of a thin lamella of glassy material (or melt phase)? with a presumably low mechanical strength (soft and ductile material) must considerably facilitate the relative shear and rotation of both sides.

Discussion

Dislocations

The following glide systems are found to be activated by the shock wave: (100)[001], {110}[001] and (100)[010]. The first one, (100)[001], is known to be the easiest glide system in a number of monoclinic pyroxenes while (100)[010] is much less usual. This glide system was, however, activated and characterized in spodumene (the C2/c pyroxene with composition $LiAlSi_2O_6$, Van Duysen et al. (1983), and in diopside (Doukhan et al. 1986) when these minerals are deformed under the severe conditions produced by room temperature indentation. The corresponding stresses and strain rates are highly heterogeneous but, in the vicinity of the indent, quite high strain rates (up to $\approx 10^{+2}\ s^{-1}$) are induced. They result from quite high deviatoric stresses (up to 1 GPa) under a confining pressure of ≈ 0.5 GPa (see review on microindentation in Westwood and Conrad (1971)). The deformation conditions induced by a shock wave are, however, still more severe and markedly larger, at least for the strain rate and the confining pressure (the level of the deviatoric stress depends on the boundary conditions and cannot be precisely estimated in shock wave experiments). It is thus not surprising that a shock wave can activate in diopside unusual glide systems with quite large elastic limits.

The phenomenon of shock-induced dislocation multiplication was already observed in shocked olivine (Ashworth and Barber 1975a, 1977; Ashworth 1985; Jeanloz et al. 1977; Jeanloz 1980). In the present case our observations clearly show that a severe dislocation multiplication occurs as the result of the activation of numerous Frank-Read sources. Every source emitted a number of loops and these loops moved over quite short distances. Their maximum flight distance can be estimated from the micrographs in measuring the distance of the most external loop to its source. This distance never exceeds a few microns (<5 µm). As the duration of the shock wave is estimated of the order of 10^{-8} to 10^{-9} s, the dislocation velocity must be of the order of $\approx 5 \cdot 10^{-6}/10^{-8} = 5 \cdot 10^{2}\ m \cdot s^{-1}$. This is quite a high and unusual velocity for dislocations in iono-covalent crystals. For comparison during usual low stress, high temperature creep tests this dislocation velocity does not exceed $10^{-9}\ ms^{-1}$. This value, however, does not exceed the

maximum theoretical velocity which would be reached under extreme deviatoric stresses, the pseudo-relativistic velocity (Hirth and Lothe 1971) $v=\sqrt{\mu/\rho}$ where μ is the shear modulus of the considered material ($\approx 7 \cdot 10^{10}$ Pa at ambient conditions) and ρ is the specific mass ($\approx 3300\ kg \cdot m^{-3}$ at ambient conditions). A rough estimate of this maximum velocity at ambient conditions yields $v=\sqrt{7 \cdot 10^{10}/3300} \approx 4.6 \times 10^3\ ms^{-1}$, a value which is only one order of magnitude larger than the measured dislocation velocity induced by the shock experiment. This very crude estimate thus suggests that, although diopside is known to be a rather ductile silicate mineral, especially at high temperature, (diopside is appreciably more ductile than quartz or feldspar at similar temperatures) quite large deviatoric stresses developed in this shock experiment which induced a large and pervasive density of dislocations by activating several glide systems. Under these conditions it is remarkable that no evidence of the activity of the glide system $^1/_2<110>\{110\}$ is found although this glide system is the one most easily activated by conventional deformation creep tests at low strain rate and high temperature (above $T \approx$ 1100° C, see Raterron and Jaoul (1991), Ingrin et al. (1991)). An inversion of competence of the various glide systems must thus occur in diopside when the strain rate is dramatically increased. This inversion of competence could result either from a marked difference in the deformation temperature which would be appreciably lower in the shock experiment (but such an assumption does not appear consistent with the observation of melt pockets) or from contrasted friction forces suffered by the various dislocation types as the strain rate is drastically increased (the strain rate in the shocked crystal is most probably larger by at least 10 orders of magnitude than the one produced by low stress, high temperature creep experiments).

Twins

Twinning is one of the relevant defects in shocked diopside, but contrasted twin configurations have been reported so far. In the present study we observe a large density of (100) twins while the (001) twins are much less numerous. In contrast Hornemann and Müller (1971) observed predominant (001) twins in experimentally shocked diopside but it should be noted that these various experiments correspond to different shock compressions. Indeed Hornemann and Müller (1971) tested the [010] and [001] shock directions while the experiments reported here correspond to a shock direction perpendicular to the (100) plane. This comparison suggests that the deviatoric stresses accompanying the shock wave which are the stresses relevant for activating mechanical twinning, must be quite large. Stöffler (1972) reports the occurrence of numerous (001) twin lamellae in a heavily naturally shocked lunar basalt while Ashworth (1985) detects similar densities of both types of twin lamellae in L-group chondrites. In meteoritic pyroxenes, either only (100) twins (mildly shocked meteorites, Ashworth 1980) or both types (weakly shocked lunar augite and Shergotty meteorite, Nord and McGee (1979), Müller (1993), respectively)) were found to occur. Such contrasting observations suggest that shock temperature and peak pressure might not be the only factors controlling the production rate of one or the other type of twins in diopside; the crystalline orientation as well as the intensity of the deviatoric stresses accompanying the shock wave might also be relevant factors. This suggestion is supported by the results of Kirby and Christie (1977) who investigated the mechanisms by which mechanical twinning occurs in diopside (it should be remembered, however, that their deformation conditions correspond to a regime of very low strain rate as compared to case of shock-induced deformation). These authors show that (100) twin lamellae result from the nucleation and the motion of partial $^1/_2$c dislocations gliding in adjacent (100) planes under the action of a deviatoric stress in the (100) plane in the [001] direction. Such a model probably holds in the present case because we observe a number of such partial dislocations in the twin boundaries. Kirby and Christie (1977) propose a similar dislocation mechanism for the production of (001) twins but in contrast with the previous case we observe no partial dislocations in the boundaries of the (001) twin lamellae. Our observations are rather consistent with the model proposed by Ashworth (1985) who suggests that for extreme conditions like the ones induced by shock waves, (001) twinning occurs by an abrupt "flipping" of an entire crack-bounded lamellar region inclusive its pre-existing substructure. This mechanism require a simultaneous cooperative motion of atoms constituted the twin lamellae. Such a "flipping" process is illustrated on Fig. 8c where the PDFs running in the $(33\bar{1})$ plane are deflected by the (001) twin lamellae which intersect them. This configuration shows clearly that the twinning process post-date the formation of the PDFs, as a consequence partial dislocations motion could not be possible through the PDFs (which consist of amorphous lamellae). Hornemann and Müller (1971), based on TEM studies of experimentally shocked diopside, report on similar (001) twin configurations, as well as Müller (1993) investigating clinopyroxene in a shocked Shergotty meteorite. Such twin lamellae are interpreted as an unequivocal effect of shock deformation. The model of Kirby and Christie for the formation of (001) twin lamellae was developed for low strain rates and it can be applied only to such situations, but not to the higher strain rates of a shock wave. It is certainly the reason why such (001) twins are found in shock-loaded rocks where stresses are very high.

Melt Pockets and Veins

Some amount of amorphized material is often found in shocked minerals and this is considered by a number of authors as important information about the intensity of the shock (Dodd and Jarosewich 1979; Stöffler et al. 1991). At least two contrasting interpretations have been proposed for this amorphization. On the one hand Jeanloz et al. (1977) suggest that the amorphous material detected in monocrystalline olivine shocked at ≈ 50 GPa would result from the reversion of high pressure polymorphs. On the other hand, Schmitt and Ahrens (1989) and Stöffler et al. (1991) noted that during a shock ex-

periment the temperature can locally reach very high values and cause melting or even vaporization. As there is no clear evidence so far for phase transformations toward high pressure polymorphs in shocked diopside, we believe that the glassy areas detected in our shocked material stem from local melting due to the heating wave associated with the pressure wave. These molten regions which now appear as glass may have corresponded to regions of stress concentration where "hot spots" were generated. We also interpret the numerous bubbles seen in the glass phase as remnants of some vaporization process which accompanied the melting process. Indeed it is to be remembered that some fluid inclusions or weathering products are detected in the starting material. They may have locally reduced the melting temperature (this would be especially the case for hydrous minerals like sheets of mica for instance). It is also to be noted that the composition of the amorphous phase does not differ significantly from the one of the starting material, i.e. there is no evidence of a polymineralic melt or of an incongruent melting although diopside is known to melt incongruently (but again one time the very short duration of the heating process may have inhibited the necessary slow diffusion process which accompanies incongruent melting). Along the same lines we interpret the small crystallites detected at the rims of these amorphized regions as the result of a limited recrystallization process in a strong temperature gradient. The other glass regions, with the shape of elongated veins would also stem from localized melting but in this case the heat would have been at least partially provided by the local friction occurring along the many fractures induced by the shock wave (Kieffer 1977).

PDFs

There are many similarities (and a few differences) between the PDFs detected in experimentally shocked diopside and the ones already observed and characterized in experimentally as well as naturally shocked quartz. The formation mechanisms should thus be rather similar in both cases. In the case of quartz, a formation mechanism was recently proposed by Goltrant et al. (1992). These authors suggest that PDFs are nucleated in the few crystallographic planes along which the crystal structure is unstable under pressure (i.e. in planes where the Born criterion of stability is violated). In these planes the quartz structure which is unstable should transform into one of its high density polymorphs (coesite or stishovite). However, because of the very short duration of the shock, a reconstructive transformation is not possible and quartz would rather transform into a highly compressible amorphous phase. As soon as nucleated these amorphous domains will be produced all along the moving shock front, leading to the straight and narrow PDFs. Such amorphous lamellae should thus occur in those planes exhibiting shear instability which are close to the propagation direction of the shock wave. Furthermore, because they present a large compressibility, the formation of PDFs must decrease the large elastic energy stored in the region highly compressed by the shock wave.

We do not know at the moment if such a model also applies to shocked diopside, because we do not know if similar instabilities occur in diopside under pressure and if they would occur in those crystallographic planes which are the PDF habit planes experimentally observed in shocked diopside. However, the remarkable similarity between the fine structures of PDFs in shocked quartz and in shocked diopside strongly suggests that the same formation mechanism should operate in both crystal structures. This is the reason why in this article the straight and narrow amorphous lamellae observed in shocked diopside are called PDFs. Indeed in both cases the PDF habit planes correspond to dense planes: on the one hand the $\{10\bar{1}n\}$ rhombohedral planes in quartz with $(10\bar{1}1)$ being the densest plane of the structure and on the other hand the crystallographic planes $(33\bar{1})$, $(22\bar{1})$ (110) of the diopside structure which are quite dense planes as examplified by their high structure factors for the diffraction of electronic waves. There is however a difference between PDFs in quartz and in diopside. In shocked quartz, PDFs are dominated by the compressive component of the shock wave and display no shear character. In contrast, PDFs in diopside occur in planes at $\approx 45°$ to the propagation direction of the shock wave (47° for (110) and $(1\bar{1}0)$, 55° for $(33\bar{1})$ and $(3\bar{3}\bar{1})$, 61° for $(22\bar{1})$). Their shear character is clearly visible at intersections where either primary PDFs or twins are displaced by another generation of PDFs (see Fig. 8c for instance). Their orientation might thus be governed by the deviatoric components of the shock stress rather than by its compressive component as in the case of quartz.

Conclusion

Diopside shocked at a peak pressure of 45 GPa exhibits a high density of defects consisting of dislocations in glide configuration, mechanical twin lamellae, straight and narrow lamellae of an amorphous phase extending in a few crystallographic planes (planar deformation features) and pockets or veins of a glassy material with a composition roughly identical to the one of the diopside matrix. The process of dislocation multiplication is clearly detected (Frank-Read sources). The twin lamellae have a mechanical origin and most of them are (100) twins while the (001) twins are much less abundant. These contrasted proportions may result from the choice of the shock direction perpendicular to the (100) plane. Therefore the occurrence of one or the other type of twin in naturally shocked diopside might not be an unambiguous index of the intensity of the shock as previously proposed by some authors because the deviatoric stresses accompanying the shock wave might also be a relevant parameter for the nucleation of one or the other type. The formation mechanism proposed by Kirby and Christie (1977) probably holds for the (100) twins but not for the (001) ones. For these latter ones the model proposed by Ashworth (1985) appears more consistent with our observations. The glass pockets and the glass veins detected in our shocked sample result from localized melting ("hot spot" model). The straight and narrow planar deformation features extending in

crystallographically controlled planes seem to be an important and characteristic defect in shocked silicate minerals. In the shock experiment reported here, they appear oriented at $\approx \pm 45°$ of the direction of shock propagation and they exhibit a shear character. Apparently they can be detected only by TEM. It would be interesting to investigate the possible occurrence and the microstructures of PDFs in diopside single crystals shocked along other directions. Finally it should be mentioned that although a number of shock defects in diopside can be detected by optical or X-ray methods, their fine structure can be elucidated only by the TEM technique. This is especially true for the PDF defects which are described for the first time in this article and which could be detected only by this latter technique.

Acknowledgements. Dr. U. Hornemann (Ernst-Mach-Institut, Weil am Rhein) is gratefully acknowledged for the performance of the shock experiment. We are also indebted to Prof. Dr. W. Hofmann and Dr. P. Seidel (Institut für Mineralogie, Münster) for providing access to the X-ray facilities. This work was supported by CNRS-INSU-DBT 'Changements de l'environnement global dans le passé', Contribution n°645.

References

Ashworth JR (1980) Deformation mechanisms in mildly shocked chondritic diopside. Meteoritics 15:105–115

Ashworth JR (1985) Transmission electron microscopy of L-group chondrites, I: Natural shock effects. Earth Planet Sci Lett 73:17–32

Ashworth JR, Barber DJ (1975a) Electron petrography of shock-deformed olivine in stony meteorites. Earth Planet Sci Lett 27:43–50

Ashworth JR, Barber DJ (1975b) Electron petrography of shock effects in a gas-rich enstatite-achondrite. Contrib Mineral Petrol 49:149–162

Ashworth JR, Barber DJ (1977) Electron microscopy of some stony meteorites. Phil Trans R Soc Lond A 286:493–506

Ashworth JR, Schneider H (1985) Deformation and transformation in experimentally shock-loaded quartz. Phys Chem Minerals 11:241–249

Christie JM, Ardell AJ (1976) Deformation structures in minerals. In: Electron Microscopy in Mineralogy (HR Wenk ed) Springer-Verlag, New York, pp 374–403

Coe R, Kirby SH (1975) The orthoenstatite to clinoenstatite transformation mechanism by shearing and its reversion by annealing: mechanism and potential applications. Contrib Mineral Petrol 52:29–55

Dodd RT, Jarosewich E (1979) Incipient melting in and shock classification of L-group chondrites. Earth Planet Sci Lett 44:335–340

Doukhan JC, Doukhan N, Nazé L, Van Duysen JC (1986) Défauts de réseau et plasticité cristalline dans les pyroxènes: une revue. Bull Minéral 109:377–394

Goltrant O, Cordier P, Doukhan JC (1991) Planar deformation features in shocked quartz; a transmission electron microscopy investigation. Earth Plan Sci Lett 106:103–115

Goltrant O, Leroux H, Doukhan JC, Cordier P (1992) Formation mechanisms of planar deformation features in shocked quartz. Phys Earth Planet Inter 74:219–240

Gratz A (1984) Deformation in laboratory-shocked quartz. J Non Crystal Sol 67:543–558

Gratz AJ, Tyburczy J, Christie JM, Ahrens TJ, Pongratz P (1988) Shock metamorphism of deformed quartz. Phys Chem Minerals 16:221–233

Grieve RAF, Sharpton VL, Stöffler D (1990) Shocked minerals and the K/T controversy. EOS Nov 13:1792

Hirth JP, Lothe J (1968) Theory of dislocations. McGraw Hill, pp 153–160

Hornemann U, Müller WF (1971) Shock-induced deformation twins in clinopyroxene. Neues Jahrb Mineral Monatsh 6:247–255

Ingrin J, Doukhan N, Doukhan JC (1991) High temperature deformation of diopside single crystals. II TEM investigation of the defect microstructure. J Geophys Res 96:14287–14297

Jeanloz R, Ahrens TJ, Lally JS, Nord GL, Christie JM, Heuer AH (1977) Shock-produced olivine glass: first observation. Science 197:457–459

Jeanloz R (1980) Shock effects in olivine and implications for Hugoniot data. J Geophys Res 85:3163–3176

Kieffer SW, Phakey PP, Christie JM (1976) Shock processes in porous quartzite: transmission electron microscope observations and theory. Contrib Mineral Petrol 59:41–93

Kieffer SW (1977) Impact conditions required for formation of melt by jetting in silicates. In "Impact and explosion cratering" (eds DJ Roddy, RO Pepin and RB Merrill) Pergamon Press 751–769

Kirby SH, Christie JM (1977) Mechanical twinning in diopside $Ca(Mg,Fe)Si_2O_6$: structural mechanisms and associated crystal defects. Phys Chem Minerals 1:137–163

Kirby SH (1976) The role of crystal defect in the shear-induced transformation of orthopyroxene to clinopyroxene. In: Wenk R (ed) Electron microscopy in mineralogy. Springer-Verlag, New York, pp 465–472

Klug HP, Alexander LF (1974) X-Ray diffraction procedures. J Wiley New York

Langenhorst F, Deutsch A, Stöffler D, Hornemann U (1992) Effect of temperature on shock metamorphism of single-crystal quartz. Nature 356:507–509

Liu LG (1987) New silicate perovskites. Geophys Res Letters 14:1079–1082

Medenbach O (1985) A new microdiffractometer spindle stage and its application. Fortschr Min 63:111–133

Müller WF (1993) Thermal and deformation history of the Shergotty meteorite deduced from clinopyroxene microstructure. Geochim Cosmochim Acta 57:4311–4322

Nord GL, McGree JJ (1979) Thermal and mechanical history of granulated norite and pyroxene anorthosite clasts in breccia 73255. Proc 10th Lunar Planet Sci Conf, pp 817–832

Raterron P, Jaoul O (1991) High temperature deformation of diopside single crystals. I. Mechanical data. J Geophys Res 96:14277–14286

Schaal RB (1982) Disequilibrium features in experimentally shocked mixtures of olivine plus silica glass powders. Contrib Mineral Petrol 81:39–47

Schmitt DJ, Ahrens TJ (1989) Shock temperatures in silica glass: implications for modes of shock-induced deformation, phase transformation, and melting with pressure. J Geophys Res 94:5851–5871

Schneider H, Vasudevan R, Hornemann U (1984) Deformation of experimentally shock-loaded quartz powders: X-ray line broadening studies. Phys Chem Minerals 10:142–147

Stöffler D (1972) Deformation and transformation of rock-forming minerals by natural and experimental shock process I. Behaviour of minerals under shock compression. Fortschr Mineral 49:50–113

Stöffler D, Keil K, Scott ERD (1991) Shock metamorphism of ordinary chondrites. Geochim Cosmochim Acta 55:3845–3867

Svendsen B, Ahrens TJ (1983) Dynamic compression of diopside and salite to 200 GPa. Geophys Res Letters 10:501–504

Svendsen B, Ahrens TJ (1990) Shock-induced temperature of $CaMgSi_2O_6$. J Geophys Res 95:6943–6953

Van Duysen JC, Doukhan N, Doukhan JC (1983) Room temperature microplasticity of α spodumene. Phys Chem Minerals 10:125–135

Westwood JH, Conrad H (1971) The science of hardness and its research applications. Amer Soc Metals Metals Park